Defects generated by misfit strain in SiGe/Si(001)

Yusuf Atici
Atatürk Üniversitesi, K. K. Egitim Fakültesi, Fizik Bölümü, Erzurum, Turkey
(Received 2 June 1994; revised manuscript received 30 August 1994)

The structure of misfit dislocations in a $Si_{0.67}Ge_{0.33}$/Si(001) strained-layer superlattice by transmission electron microscopy (TEM) has been analyzed. An orthogonal set of misfit dislocations, using plan-view TEM specimens, was observed at the strained-layer interfaces relaxing the strain in the structure. Conventional **g**·**b** diffraction contrast experiments displayed 60°-type misfit dislocations with $a/2\ \langle 100 \rangle$ $\{111\}$ slip system. To observe the propagation and generation of misfit dislocations in the superlattice, a number of annealing experiments were carried out in a vacuum furnace at temperatures between 550 and 1050 °C at a pressure of 1×10^{-6} Torr for 5 min. The experimental study was performed in the microscope taking micrographs before and after each annealing process. Consequently, two orthogonal sets of misfit dislocations were generated in the superlattice at two different temperatures (760 and 940 °C). It was ascertained that the first set of dislocations is generated by the threading dislocations and the second set is produced by the structure. An interstitial type of dislocation loop was attained for the dislocation generation mechanism at high temperatures.

I. INTRODUCTION

Recently, $Si_{1-x}Ge_x$ films on Si substrates grown by molecular-beam epitaxy (MBE) have been found to be important in semiconductor device technology. The interest in applying SiGe strained layers in semiconductor devices arises from the fact that the incorporation of germanium in silicon films causes a reduction of the band gap because of the presence of compressive strain in the epitaxial layer.[1,2] There have been many attempts to grow defect-free Ge and SiGe films on Si substrates. However, it has been observed that the structures had many defects in the epilayers, epilayer-substrate interfaces, and substrates such as rough interfaces caused by three-dimensional growth, cracks, precipitates, misfit and threading dislocations, and stacking faults.[3–9]

It is not yet possible to grow defect-free SiGe films on Si substrates that have a significant lattice misfit strain relative to the substrate even by crystal-growth techniques such as MBE and metal-organic vapor-phase epitaxy (MOVPE). The lattice mismatch between Si and $Si_{1-x}Ge_x$ layers can be accommodated by tetragonal distortion of the alloy layer, introducing strain into the lattice.[10–12] This strain can mainly affect the optical and electrical characteristics of the material, allowing so-called band-gap engineering to tailor these properties for specific applications, for example, IR photodetectors, modulation-doped field-effect transistors, resonant-tunneling diodes, and other integrated electro-optical devices for telecommunications.

The strain introduced by the lattice mismatch is crucial for device performance, and therefore any nonuniformities in strain cannot be tolerated.[11] If the film thickness exceeds a certain critical thickness (h_c) for a given $Si_{1-x}Ge_x$ composition, the strain energy incorporated into the lattice can cause a partial or complete relaxation, with the alloy layer returning to its original lattice parameter. The critical thickness for $Si_{1-x}Ge_x$/Si heterostructures depends upon x.[8,13–16] For example, $h_c=100$ Å for $Si_{0.5}Ge_{0.5}$ on the Si(100) buffer layer, and for the lattice mismatch inherent to potentially important combinations such as GaAs/Si and Ge/Si ($\varepsilon\sim4\%$) the critical thickness $h_c(\varepsilon)$ is approximately 10 Å. For epilayer thicknesses greater than these values misfit dislocations occur at the substrate-epilayer interface, and relax strain energy in the epilayer. These misfit dislocations, and especially the threading dislocations connecting the misfit dislocations to the growth surface, can seriously affect the electrical and optical properties. Indeed, the formation and propagation of misfit dislocations in strained materials can dramatically expand opportunities for combining materials such as Si and Ge that have a 4% lattice mismatch.[1,9] However, to access the promise of the SiGe system fully, thick, relaxed SiGe films on Si substrates without threading dislocations would have to be grown. This is a very provocative problem, because the relaxation mechanism involves the motion of threading dislocations through the film.

In this study, a $Si_{0.67}Ge_{0.33}$/Si(001) superlattice was examined by transmission electron microscopy. In order to analyze the defects in plan-view samples, **g**·**b** analysis, stereo microscopy, diffraction contrast experiments, and high-temperature heat treatments were used.

II. EXPERIMENT

The $Si_{0.67}Ge_{0.33}$/Si(001) superlattice was grown by MBE at 550 °C. The mismatch between the epilayer and substrate is 1.378%. The strained-layer superlattice (SLS) has 21 repeated SiGe layers with a thickness of

 ©1995 The American Physical Society

~200 Å. The thickness of the Si layer in the periodic structure is about 450 Å. Plan-view TEM specimens were prepared by back-thinning from the substrate side mechanically and chemically using a solution of 17% HF and 83% HNO_3 or $CH_3COOH:HNO_3:HF=1:2:1$. A Philips EM430 electron microscope, operating at a voltage up to 250 kV, was used to carry out the diffraction contrast experiments. In order to prevent problems associated with the hot stage in the microscope, such as a broken sample after using the microscope as a result of sticking of the sample and sample holder, lack of a double tilt specimen holder, contamination, etc., the annealing processes were done using a vacuum furnace. The applicable maximum temperature is 1200 °C in the furnace. Before the initial annealing process, electron micrographs from an area in a plan-view TEM sample were taken in different reflections in the microscope. Thereafter the sample was put in a crucible boat for the annealing process. The crucible boat with the specimen was placed into the crucible specimen chamber of the furnace. In order to prevent contamination, annealing experiments were carried out in the furnace at temperatures between 550 and 1050 °C at a pressure of 1×10^{-6} torr for 5 min. The annealing processes were done stage by stage. Following each stage, the sample was examined in the microscope. Although the specimen came off from the slot grid after each annealing stage in the furnace, the use of the vacuum furnace provided a very good opportunity in this study to obtain good results from the interfacial defects.

III. RESULTS

A. Observation of misfit and threading dislocations in plan-view samples

Since there is a mismatch ($\eta=1.3785\%$) between silicon substrates and $Si_{0.67}Ge_{0.33}$ films, the misfit dislocations are generated at the interfaces (or around the interfaces), relaxing the strain in the structure. Figure 1 presents a TEM micrograph of these misfit dislocations in a plan-view SiGe/Si(001) specimen. The misfit dislocations in the micrograph run in the [110] and $[1\bar{1}0]$ directions, lying in a (001) plane parallel to the surface of the wafer and thus forming an orthogonal set. These dislocation lines are expected to run along the interfaces to the edge of the wafer. If they end in the interfacial plane they thread to the wafer surface, forming threading dislocations, or may annihilate with other dislocations of the same Burgers vector.[14,17]

Figure 1 shows that the dislocation lines have some point contrast features on and at the end of them (indicated by arrows). This indicates that the dislocations run along the interface for a distance, though not to the edge of wafer. Figure 2 shows a pair of stereomicrographs that show that these point contrast features represent dislocations in the epilayers (the micrographs were taken in $\mathbf{g}=\bar{2}20$ with an angle of ~5° away from both sides of the [001] zone axis). These are threading dislocations. The misfit dislocations thread from one interface to another at these points, generating other misfit dislocations [further work is being carried out on these threading segments and the misfit dislocation interactions in plan-view $Si_{0.67}Ge_{0.33}$/Si(001) samples]. However, there are misfit dislocations that can be seen in Fig. 1 that have slightly rounded tips turning away from the ⟨110⟩ directions. This might be due to the local climb processes.[18]

B. The g·b analysis of dislocations

The visibility of misfit dislocations in SiGe/Si can be understood in terms of the simple $\mathbf{g}\cdot\mathbf{b}$ criterion. For the determination of the Burgers vector of a dislocation, two diffracting vectors $\mathbf{g}_1$ and $\mathbf{g}_2$ are found in which the dislocation is invisible then $\mathbf{b}=\mathbf{g}_1\times\mathbf{g}_2$.[19–22]

The micrographs in Fig. 3 have been taken under a two-beam condition from the same area seen in Fig. 2 using 3g [weak-beam (WB) along $\mathbf{g}=\bar{2}20$], $\mathbf{g}=\bar{4}00$ and $\mathbf{g}=111$. The misfit dislocations are visible in $\mathbf{g}=\bar{2}20$ and 3g. Some of them (indicated in the WB picture) are invisible in $\mathbf{g}=\bar{4}00$ and $\mathbf{g}=111$, therefore b is found for these dislocations to be $\mathbf{b}=\pm a/2[0\bar{1}1]$.

More experimental work has been done on the same material using different specimens, and similar types of Burgers vectors have been found which were also $a/2\langle110\rangle$ types. In order to show the dislocation slip systems, the results have been shown in a stereographic projection in Fig. 4. All the results obtained are depicted

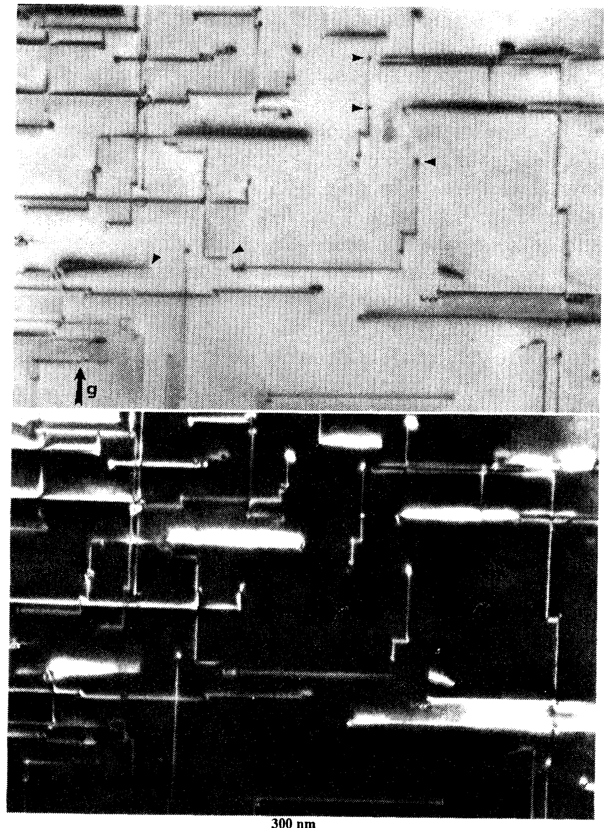

FIG. 1. A pair of bright- and dark-field micrographs taken in $\mathbf{g}=2\bar{2}0$, displaying a general view of the orthogonal misfit dislocations in a plan-view sample of SiGe/Si SLS.

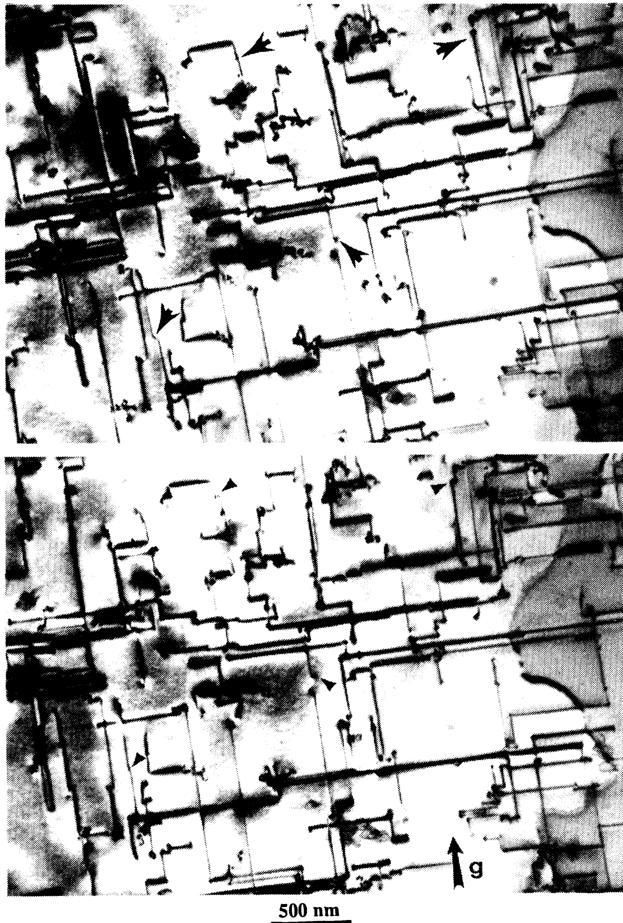

FIG. 2. A pair of stereomicrographs taken in $\mathbf{g}=\bar{2}20$, demonstrating that the dots on the misfit dislocation lines represent the threading dislocations in the superlattice.

in Table I. In this study, it was found that the misfit dislocations in the $Si_{0.67}Ge_{0.33}$/Si(001) superlattice had $a/2\langle 110\rangle\{111\}$ slip systems.

C. Dislocation configurations at high temperatures

SiGe films grown by MBE on Si substrates are deposited at low temperatures (~500 °C) to prevent the relaxation of strain by diffusion or dislocation formation. Integration of such a metastable layer in a device structure needs several processing stages such as selective etching, implantation, oxide deposition and thermal activation.[2] The typical temperature range of these steps is between 600 and 900 °C. Hence the thermal stability of strained layers in terms of diffusion and relaxation is very important.

In order to observe the migration and generation of misfit dislocations in the $Si_{0.67}Ge_{0.33}$/Si(001) superlattice, a number of annealing experiments were performed in a vacuum furnace at temperatures between 550 and 1050 °C at a pressure of 1×10^{-6} Torr for 5 min. Plan-view speci-

TABLE I. Burgers vectors (**b**), line directions (**u**), and possible planes for the observed misfit dislocations in the plan-view samples of the superlattice.

b	**u**	Plane
$a/2[101]$	$[\bar{1}10]$	$(\bar{1}\bar{1}1)$
	$[110]$	$(\bar{1}11)$
$\pm a/2[\bar{1}01]$	$[\bar{1}10]$	(111)
	$[110]$	$(1\bar{1}1)$
$\pm a/2[01\bar{1}]$	$[\bar{1}10]$	(111)
	$[110]$	$(\bar{1}11)$
$\pm a/2[011]$	$[\bar{1}10]$	$(\bar{1}\bar{1}1)$
	$[110]$	$(1\bar{1}1)$

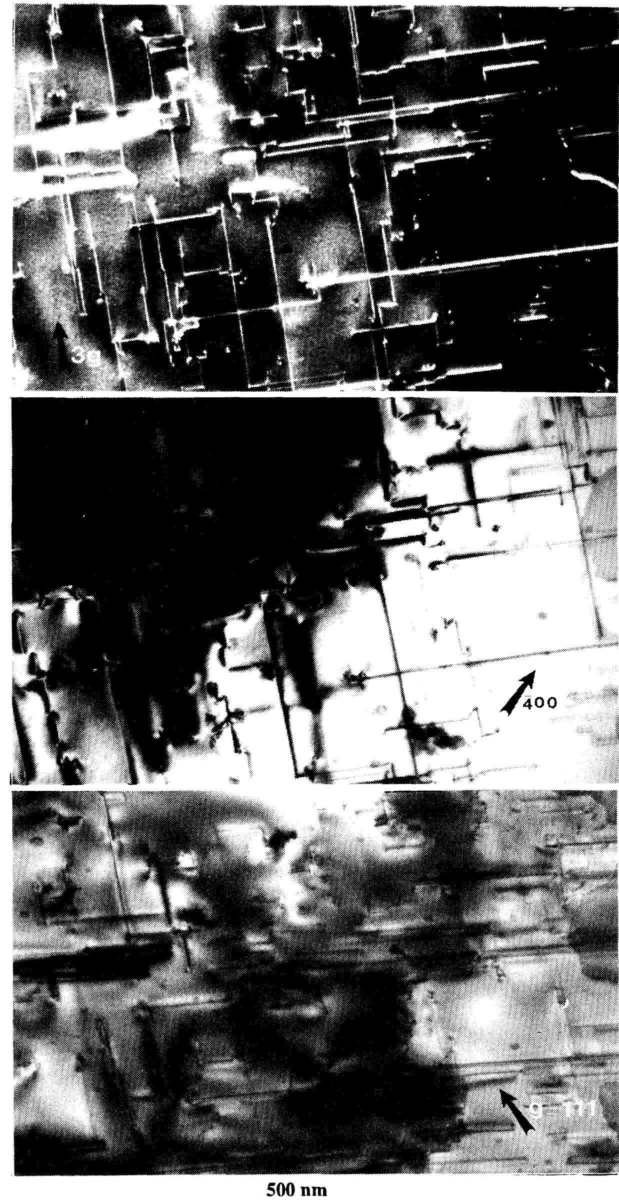

FIG. 3. Misfit dislocation contrast in different reflections for $\mathbf{g}\cdot\mathbf{b}$ analysis.

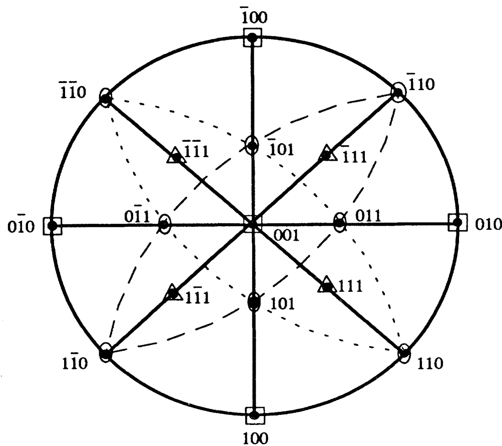

FIG. 4. A stereographic projection displaying the slip system of misfit dislocations in the superlattice.

mens with nickel or copper slot grids were subjected to these experiments. A double-tilt holder was used in the microscope for the ease of dislocation visibility and to enable a choice of any diffraction contrast. The specimens were put in a crucible boat for the annealing process in the vacuum furnace. The experimental study was carried out in the microscope, taking pictures before and after each annealing process.

The propagation and generation of dislocations were observed at a high temperature of ~760 °C. Following this, the dislocations were examined in the microscope, elevating the temperatures up to 1050 °C. A series of pictures in Fig. 5 shows how the dislocations generate and propagate in the SiGe/Si(001) superlattice at the elevated temperatures. The sample has a thickness up to 4000 Å (1-11 interfaces). No sign of dislocation generation or propagation was observed at temperatures of 550–700 °C. A slight movement of dislocations was observed at 760 and 860 °C [Figs. 5(b) and 5(c)]. The activation energy for the dislocation nucleation and migration is attained at these temperatures. The dislocation nucleation and migration in SiGe films grown on Si substrates were observed at a temperature of 700–900 °C (activation energy ~2 eV).[12,15,23–24]

It is important to note that the movements of dislocations start from the threading segments and dislocation right angle points [some are indicated in Fig. 5(a) before the hot stage was applied]. Additional dislocations were observed at 940–1050 °C [Figs. 5(d)–5(f)]. Figure 5(g) illustrates the dislocation structure in a weak beam diffraction contrast (3**g**, along the [$\bar{2}20$] Kikuchi band) at 1050 °C. In order to obtain more dislocations in different directions, a few diffraction contrast experiments were

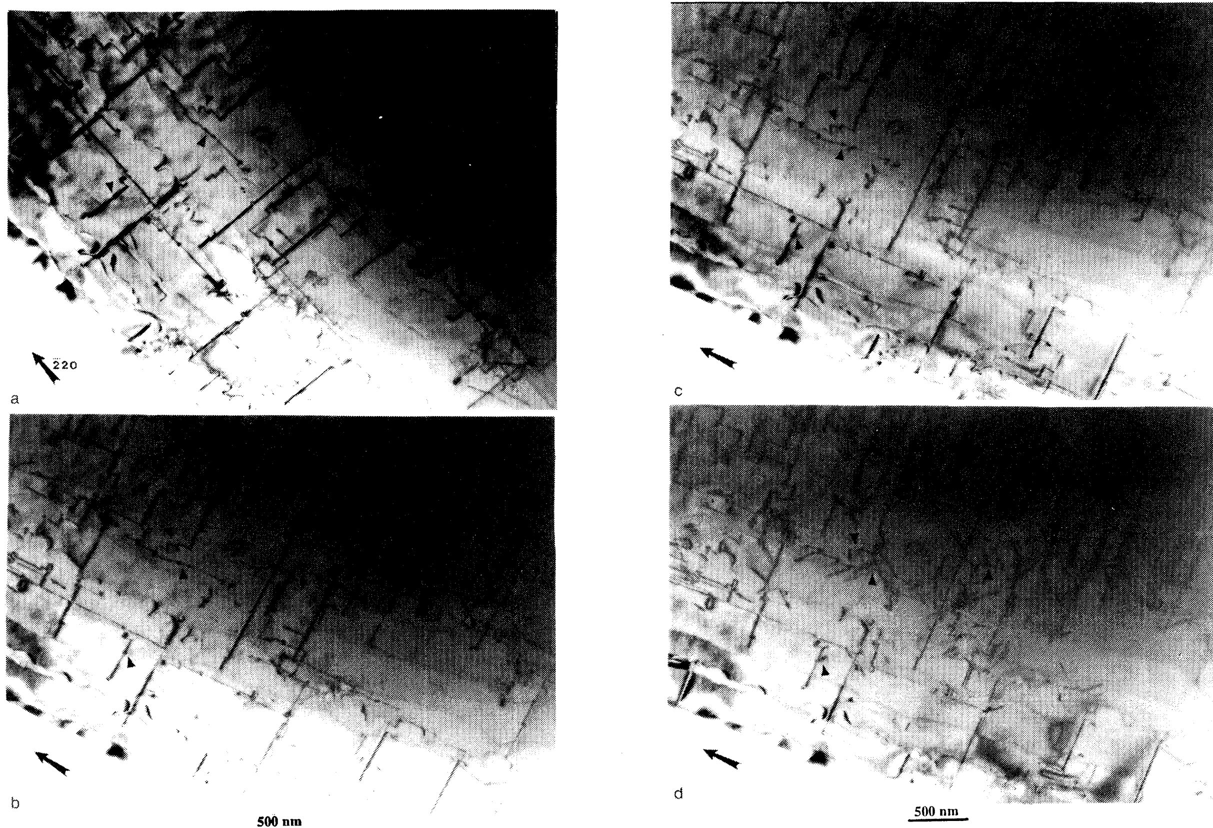

FIG. 5. A series of micrographs showing the dislocations at elevated temperatures. These temperatures are 550, 760, 860, 940, 1000, and 1050 °C for the micrographs in (a)–(f), respectively.

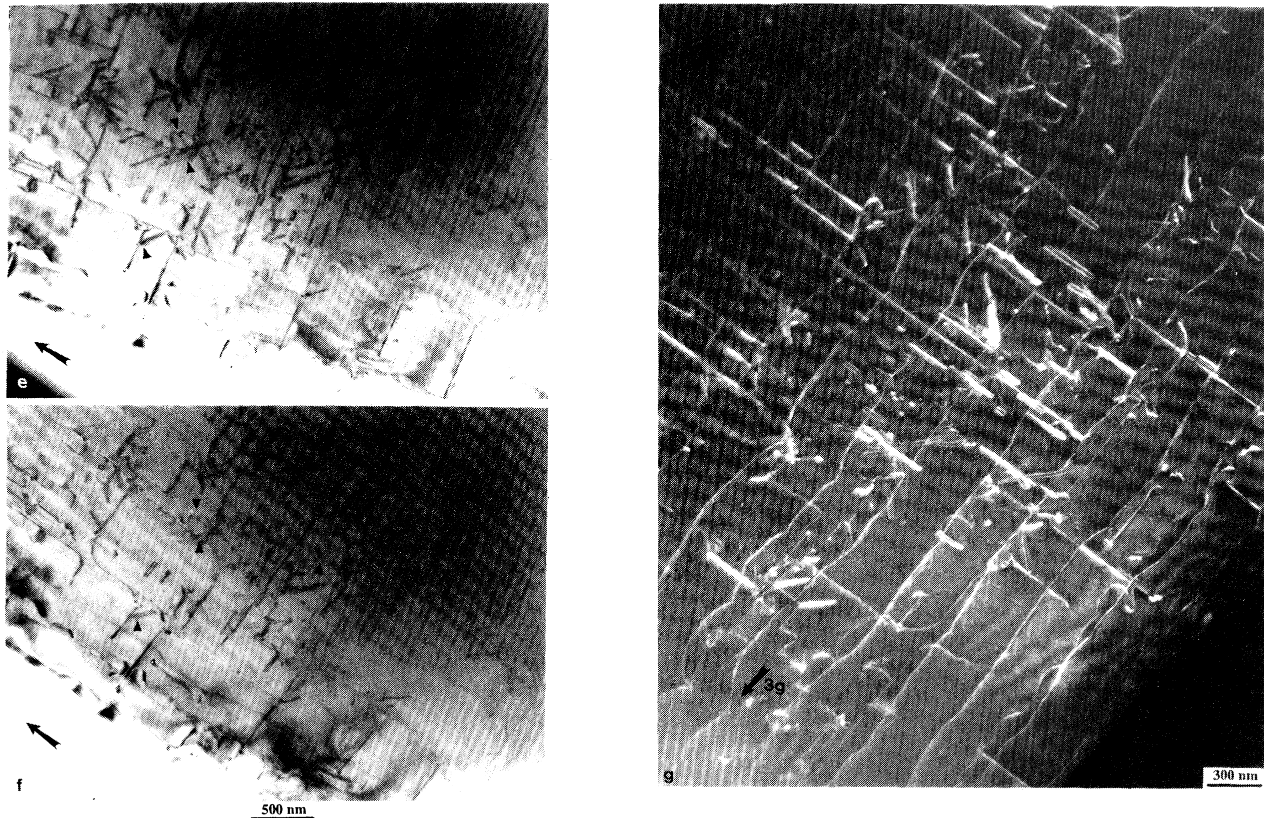

FIG. 5. (*Continued*).

carried out in the microscope, according to dislocation visibility. Figure 6 is a bright-field image of the same area seen in Fig. 5, taken in $\mathbf{g}=\bar{2}\,\bar{2}0$ after applied a temperature of 1000 °C. The image shows dislocations lying along the $[\bar{1}10]$ direction.

As a result of annealing experiments, two orthogonal sets of dislocations were observed in the SiGe/Si(001) superlattice. For the first orthogonal set of dislocations, $\mathbf{b}=a/2[101]$- and $a/2[0\bar{1}1]$-type Burgers vectors were found. The projections of dislocations in this set are along the directions at an angle of ~45° to $[\bar{1}10]$ and [110] directions in Fig. 5. They lie on the (001) plane, having projections along ±[100] and ±[010] directions. These dislocations were produced at about 760 °C in the vicinity of threading segments and dislocation right-angle points. The Burgers vectors of the dislocations in the second set were found to be $\mathbf{b}=a/2[101]$ and $a/2[\bar{1}01]$. This set of dislocations running along [110] and $[\bar{1}10]$ was generated by the superlattice at high temperature. This means that the source of the latter dislocations is neither the misfit nor the threading dislocations that were in the superlattice before the annealing process. The dislocations in the second set have not been observed at temperatures up to 860 °C. They appeared at around 940 °C [Fig. 5(d)].

It can be suggested that dislocation generation, propagation, and interaction at high temperatures can be attributed to the dislocation climb mechanism. The climb process at high temperature can be related to motions of interstitial atoms or vacancies. In order to distinguish the source of the climb mechanism, the diffraction contrast must be considered inside and outside the dislocation loops according to the images in $\pm\mathbf{g}$ taken with the same deviation parameters $\mathbf{s}_{\mathbf{g}}$.[19,21,25] The experiment can

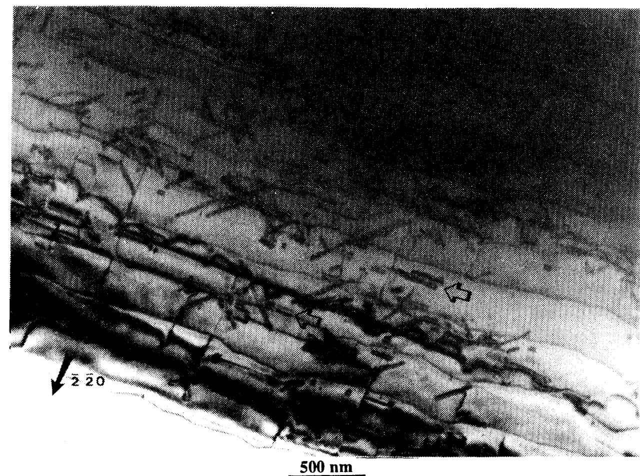

FIG. 6. An image of the misfit dislocations in $\mathbf{g}=\bar{2}\,\bar{2}0$ at 1000 °C showing the dislocations lying along $[\bar{1}10]$ (the same area seen in Fig. 5).

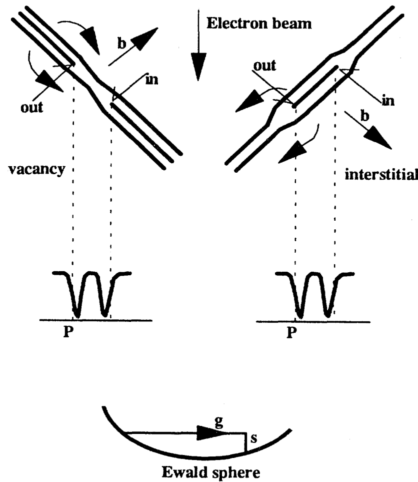

FIG. 7. A sketch showing vacancy and interstitial dislocation loops. They lie in opposite senses with respect to the thin foil surfaces. In this configuration the contrast of both loops will appear inside the actual position of the loop [Courtesy of Hirsch *et al.* (Ref. 19)].

also be done by changing the sign of **s** and keeping **g** invariant. However, the inclination of the loop plane must also be known.

As shown in Fig. 7 the contrast from the distortion of the reflecting planes lies inside the dislocation loop for the interstitial and vacancy loop for the **g** shown in the figure. If **g** is reversed the strong contrast will be outside the loop for the interstitials and vacancies. Therefore, interstitial and vacancy loops cannot be distinguished without knowing the inclination of the loop plane. This can be summarized by the rule that if $(\mathbf{g}\cdot\mathbf{b})\mathbf{s}$ is positive then the image will lie outside the loop, and if it is negative the image will be inside.

In this study, this feature of dislocation loops has been viewed in bright-field images, as seen in Fig. 8 using $\mathbf{g}=\pm\bar{2}20$ with the same deviation parameters $\mathbf{s}_g$. In the micrographs, the contrast inside and outside the loops (some are indicated) can be seen easily. This leads to whether the loop is of interstitial or vacancy type depending on the inclination of the planes involved.

The results given above have been combined with the tilt experiments in the microscope to find the mechanism of dislocation loop formation at high temperatures in the superlattice. The loops indicated in Fig. 8 are larger in $\mathbf{g}=\bar{2}20$ than in $\mathbf{g}=2\bar{2}0$, where the opposite reflection is used. Thus $\mathbf{g}\cdot\mathbf{b}<0$ for the loops since $\mathbf{s}_g$ is positive.[19,26] The Burgers vectors which satisfy the observed image contrast changes are $\mathbf{b}=a/2[011]$ (for the one with an angle of 45° to the others) and $b=a/2[101]$. Since all of these **b** are in the same sense as [001], the upward drawn normal to the foil, then the loops are interstitial.

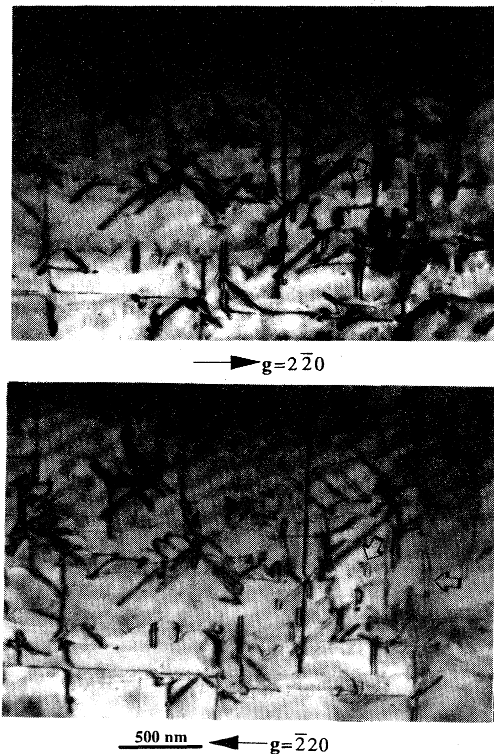

FIG. 8. Contrast inside and outside the dislocation loops in the superlattice ($\mathbf{g}=2\bar{2}0$ and $\bar{2}20$).

IV. DISCUSSION

TEM observations showed an orthogonal set of misfit dislocations in plan-view SiGe/Si(001) samples as a result of strain relaxation. The dislocations run in the [110] and [1$\bar{1}$0] directions following the interfaces with negligible height variation. Conventional $\mathbf{g}\cdot\mathbf{b}$ diffraction contrast experiments revealed the Burgers vectors of dislocations. In order to determine the value of **b**, the misfit dislocations in plan-view samples of the superlattice have been imaged in the 220-, 400-, and 111-type reflections. A clear contrast of misfit dislocations has always been observed in $\mathbf{g}=220$-type reflections which are attributed to the dislocations being of 60° type. The dislocations were invisible or had weak contrast in the other reflections. The lack of any disappearance of dislocation contrast in the reflections used prevents the determination of **b** for the misfit dislocations. The residual contrast also makes it difficult to determine the value of **b**, but the results are consistent with the interpretation that misfit dislocations were of 60° type, having $a/2\langle 110\rangle\{111\}$ slip systems.

The application of $\mathbf{g}\cdot\mathbf{b}$ has presented different types of dislocations at the epilayer-substrate interfaces. For instance, 60°-type, pure edge and mixed dislocations in $Ga_{1-x}As_xP$/GaAs, SiGe/Si, and $Cd_{1-x}Mn_xTe$/CdTe strained-layer interfaces have been observed.[6,27,28] In addition to these misfit dislocations, dislocations have been observed in SiGe/Si as a result of the dissociation of 60° misfit dislocations $(\frac{1}{2}[\bar{1}10]_{60}\rightarrow 1/6[\bar{2}1\bar{1}]_{90}+\frac{1}{6}[\bar{1}21]_{30})$.[29]

However, triple dislocation nodes can be in operation for the dislocation multiplication at the interfaces.[27,29] These nodes could inhibit the motion of dislocations and are effective in $Ga_{1-x}As_xP$/GaAs and SiGe/Si (single films on the substrates). In this study, such defects have not been observed in the SiGe/Si superlattice. It can be

emphasized that most of the dislocation sources, such as dislocation nodes, are not effective in the multilayered structures grown by MBE, e.g., $Si_{0.67}Ge_{0.33}/Si(001)$.

The investigation of dislocations in the SiGe/Si superlattice at high temperatures has presented two orthogonal sets of misfit dislocations in the structure. Most of these dislocations are in the form of loops. The first set of dislocations with $\mathbf{b}=a/2[101]$ and $a/2[0\bar{1}1]$ has been produced by threading segments, and dislocation right-angle points at around 760 °C. The second set of misfit dislocations with $\mathbf{b}=a/2[101]$ and $a/2[\bar{1}01]$ has been generated by the structure at ~940 °C. The generation mechanism of those loops could be the diffusion of either interstitial or vacancies. The most probable mechanism could be the diffusion of Ge atoms at high temperatures as observed by Fiory *et al.*[30] and Van de Walle *et al.*[2] At high temperatures such as ~800 °C, Ge diffusion becomes a dominant mechanism for strain relaxation in the epilayers. An attempt has been made with the loops to deduce the generation mechanism, and consequently the results showed that the loops are interstitial type in the strained-layer superlattice.

V. SUMMARY

The structure of interfacial defects at the interfaces of SiGe/Si(001) SLS by TEM has been studied using plan-view specimens. It was observed that the strain relaxation in 21-period $Si_{0.67}Ge_{0.33}/Si(001)$ occurs in the presence of an orthogonal set of 60°-type misfit dislocations with an $a/2\langle 110\rangle\{111\}$ slip system. As a result of annealing experiments, using a vacuum furnace, two orthogonal sets of misfit dislocations were generated into the strained-layer superlattice at two different temperatures, 760 and 940 °C. It was discovered that the first set of these dislocations is produced by the threading dislocations, and the second set is generated by the structure. The observations indicated that the dislocation loops are of an interstitial type.

ACKNOWLEDGMENTS

The author is grateful to Dr. David Cherns, Professor Cheng Tsien Chou, and Professor Andrew Lang (University of Bristol, UK) for helpful discussions and comments. The YÖK and K. Karabekir Education Faculty are acknowledged for the financial support.

[1] H. L. Fraser, D. M. Maher, C. J. Humphreys, C. J. D. Hetherington, R. V. Knoell, and J. C. Bean, in *Electron Microscopy and Analysis*, IOP Conf. Proc. No. 76 (Institute of Physics and Physical Society, London, 1985), pp. 307–312.

[2] G. F. A. Van de Walle, L. J. Van Ijzendorrn, A. A. Van Gorkum, R. A. Van den Heuvel, A. M. L. Theunissen, and D. J. Gravesteijen, Thin Solid Films **183**, 183 (1989).

[3] A. L. Aseev, O. I. Vasin, S. I. Stenin, N. N. Soldatenko, and Y. A. Tkhorik, Thin Solid Films **30**, 73 (1975).

[4] E. Kasper and H. J. Herzog, Thin Solid Films **44**, 357 (1977).

[5] B. S. Meyerson, K. J. Uram, and F. K. LeGoues, Appl. Phys. Lett. **53**, 25 (1988); **53**, 2555 (1988).

[6] D. D. Perovic, G. C. Weatherly, and D. C. Houghton, in *Evaluation of Advanced Semiconductor Materials by Electron Microscopy,* edited by D. Cherns (Plenum, New York, 1989), pp. 355–357.

[7] D. J. Eaglesham, E. P. Kvam, D. M. Maher, C. J. Humphreys, and J. C. Bean, Philos. Mag. A **59**, 5 (1989); **59**, 1059 (1989).

[8] R. Hull, R. E. Leibenguth, and D. J. Werder, J. Appl. Phys. **65**, 12 (1989); **65**, 4723 (1989).

[9] F. K. LeGoues, B. S. Meyerson, and J. F. Morar, Phys. Rev. Lett. **66**, 22 (1991); **66**, 2903 (1991).

[10] J. C. Bean, L. C. Feldman, A. T. Fiory, S. Nakahara, and I. K. Robinson, J. Vac. Sci. Technol. A **2**, 2 (1984); **2**, 436 (1984).

[11] W. J. Rothwell, S. T. Davey, B. Wakefield, C. J. Gibbings, and C. G. Tuppen, in *Electron Microscopy and Analysis,* IOP Conf. Proc. No. 100 (Institute of Physics and Physical Society, London, 1989), pp. 253–258.

[12] R. Hull, J. C. Bean, D. Bahnack, and C. Buescher, in *Evaluation of Advanced Semiconductor Materials by Electron Microscopy* (Ref. 6), pp. 381–394.

[13] A. T. Fiory, J. C. Bean, L. C. Feldman, and I. K. Robinson, J. Appl. Phys. **56**, 4 (1984); **56**, 1227 (1984).

[14] R. People and J. C. Bean, Appl. Phys. Lett. **47**, 3 (1985); **47**, 322 (1985).

[15] B. W. Dodson and J. Y. Tsao, Appl. Phys. Lett. **51**, 17 (1987); **51**, 1325 (1987).

[16] R. Hull, J. C. Bean, D. J. Eaglesham, J. M. Bonar, and C. Buescher, Thin Solid Films **183**, 117 (1989).

[17] J. W. Matthews and A. E. Blakeslee, J. Cryst. Growth **27**, 118 (1974).

[18] H. Strunk, W. Hagen, and E. Bauser, Appl. Phys. **18**, 67 (1979).

[19] P. B. Hirsch, A. Howie, R. B. Nicholson, D. W. Pashley, and M. J. Whelan, *Electron Microscopy of Thin Crystals* (Spottiswoode, Ballantyne & Co., Ltd., London, 1965).

[20] G. Thomas and J. J. Goringe, *Transmission Electron Microscopy of Materials* (Tech, 1979).

[21] M. H. Loretto, *Electron Beam Analysis of Materials* (Chapman and Hall, London, 1984).

[22] D. Hull and D. J. Bacon, *Introduction to Dislocations* (Pergamon, New York, 1984).

[23] R. J. Hauenstein, R. H. Miles, E. T. Croke, and C. McGill, Thin Solid Films **183**, 79 (1989).

[24] S. M. Jang and H. W. Kim, Appl. Phys. Lett. **61**, 3 (1992); **61**, 315 (1992).

[25] D. Cherns, P. Hirsch, and H. Saka, Proc. R. Soc. London Ser. A **371**, 213 (1980).

[26] D. J. Mazey, R. S. Barnes, and A. Howie, Philos. Mag. **7**, 1861 (1962).

[27] M. S. Abrahams, L. R. Weisberg, C. J. Buiocchi, and J. Blanc, J. Mater. Sci. **4**, 223 (1969).

[28] S. J. Diamond, Ph.D. thesis, University of Bristol, UK, 1991.

[29] K. Rajan and M. Denhoff, J. Appl. Phys. **62**, 5 (1987); **62**, 1710 (1987).

[30] A. T. Fiory, J. C. Bean, R. Hull, and S. Nakahara, Phys. Rev. B **31**, 6 (1985); **31**, 4063 (1985).

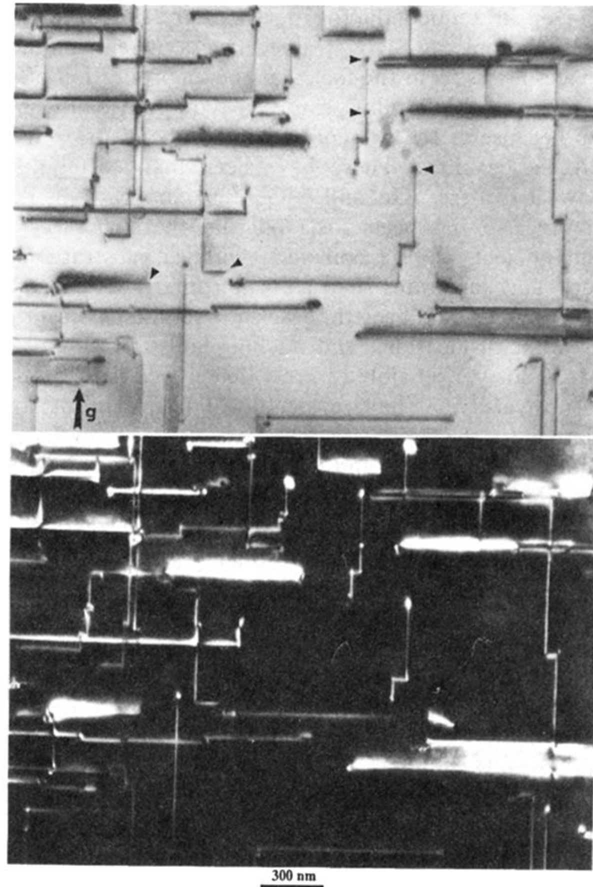

FIG. 1. A pair of bright- and dark-field micrographs taken in $\mathbf{g}=2\bar{2}0$, displaying a general view of the orthogonal misfit dislocations in a plan-view sample of SiGe/Si SLS.

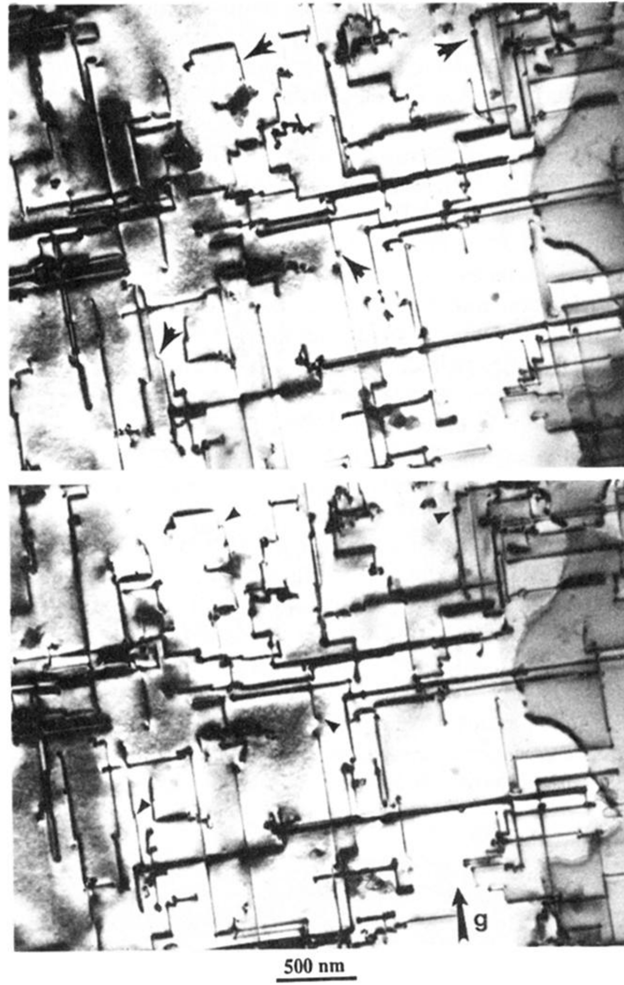

FIG. 2. A pair of stereomicrographs taken in $\mathbf{g}=\bar{2}20$, demonstrating that the dots on the misfit dislocation lines represent the threading dislocations in the superlattice.

FIG. 3. Misfit dislocation contrast in different reflections for **g**·**b** analysis.

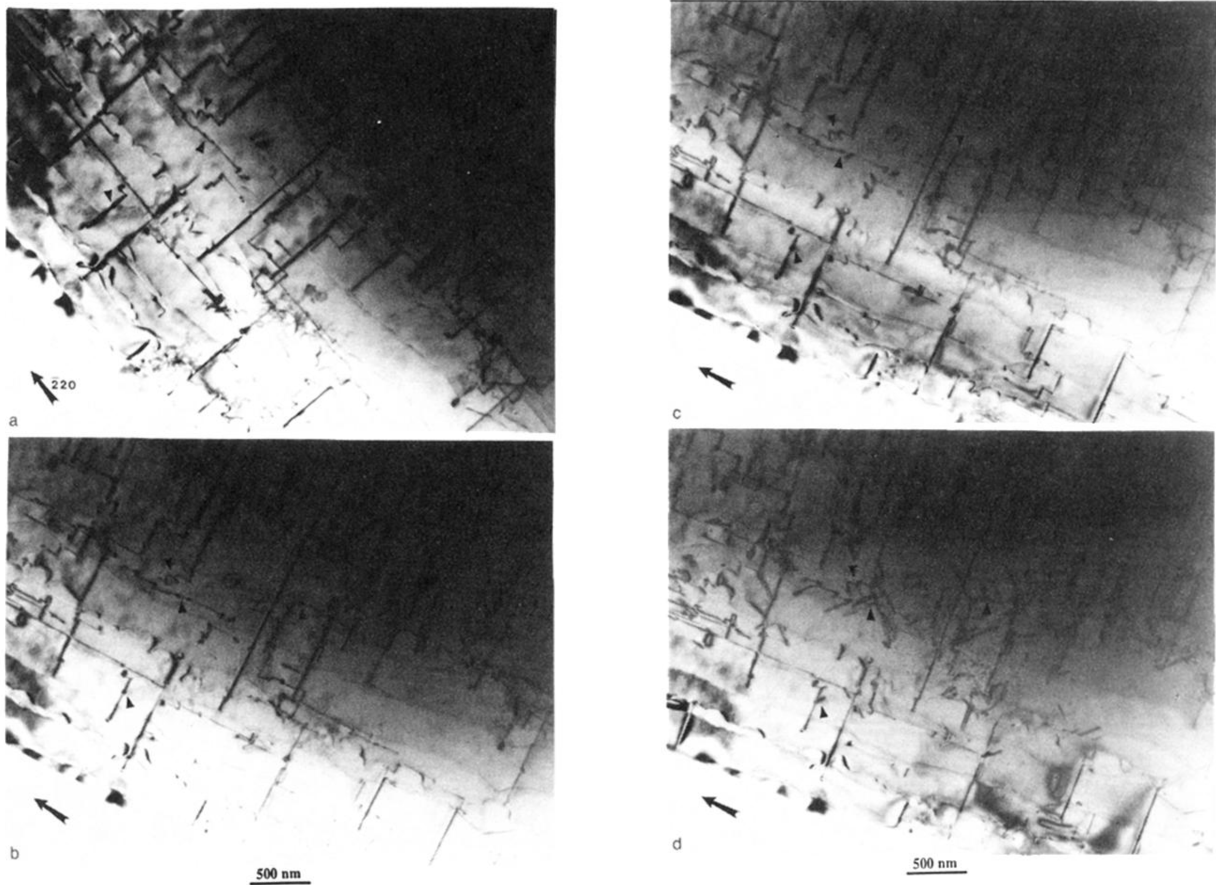

FIG. 5. A series of micrographs showing the dislocations at elevated temperatures. These temperatures are 550, 760, 860, 940, 1000, and 1050 °C for the micrographs in (a)–(f), respectively.

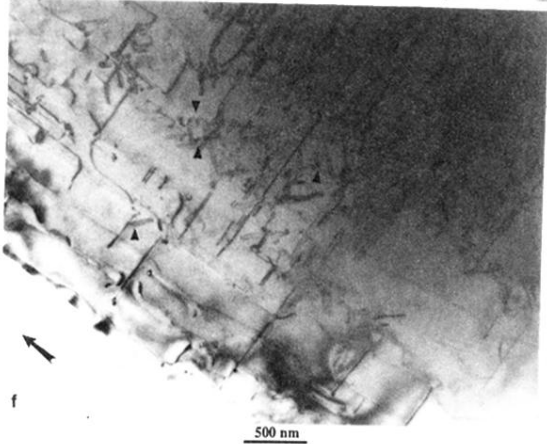

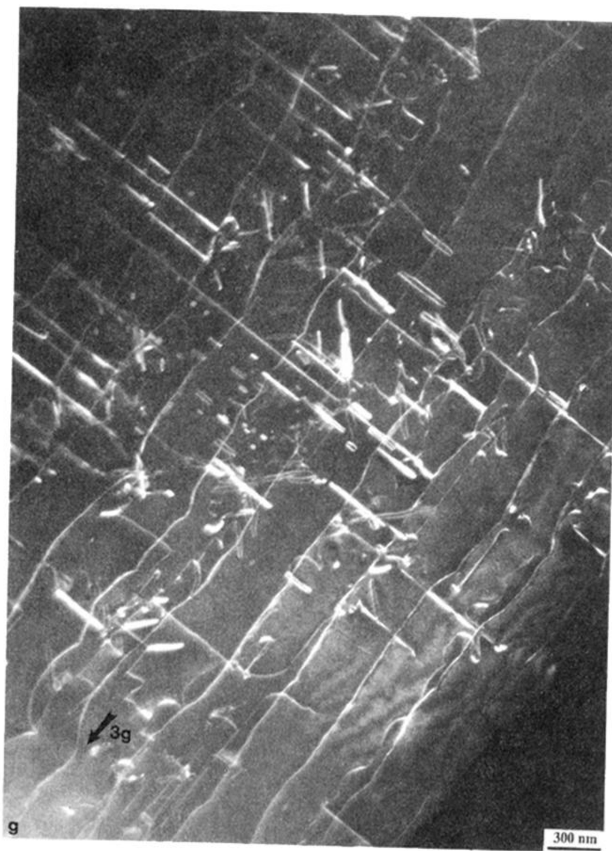

FIG. 5. (*Continued*).

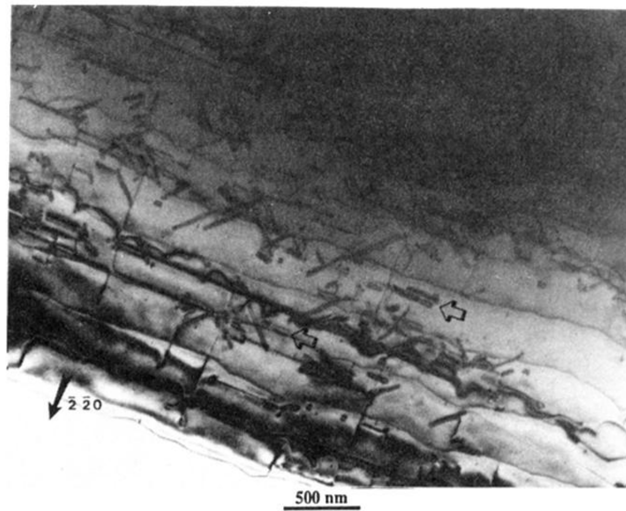

FIG. 6. An image of the misfit dislocations in $\mathbf{g}=\bar{2}\bar{2}0$ at 1000 °C showing the dislocations lying along $[\bar{1}10]$ (the same area seen in Fig. 5).

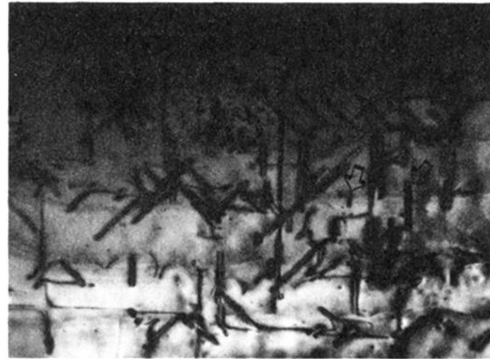

$\mathbf{g}=2\bar{2}0$

500 nm $\mathbf{g}=\bar{2}20$

FIG. 8. Contrast inside and outside the dislocation loops in the superlattice ($\mathbf{g}=2\bar{2}0$ and $\bar{2}20$).